

INVESTIGATING DISK DISSIPATION: THE CASE OF CQ TAU AND MWC 758

Chapillon, E.^{1,2,3}, Guilloteau, S.^{1,2}, Dutrey, A.^{1,2} and Piétu, V.³

Abstract. The Herbig Ae stars are the massive analogs of the TTauri stars. Very few disks surrounding these kind of stars have been studied in detail. To better constraint the disks parameters (temperature and density) we observed the disks around CQ Tau and MWC 758 with the IRAM array in continuum and CO line emissions. The disks properties are derived using a standard parametric model. The two sources show a surprising low CO abundance (assuming a standard gas-to-dust ratio). We use the Meudon PDR code to study the chemistry. For CQ Tau we find that photodissociation of CO is a viable mechanism to explain the CO depletion without modifying the gas-to-dust ratio. However, we find in both sources that the temperature of large grains can be low enough to prevent CO from being released from the grain surfaces. In addition the low inclination of the CQ Tau disk challenges the UX Ori classification of this star. We conclude that CO does not appear as a direct tracer of the gas-to-dust ratio.

1 Introduction

Planetary formation takes place in the protoplanetary disks of gas and dust surrounding young stars. However, the overall properties of these disks are not yet well constrained by current observations. It is now generally admitted that the disks surrounding intermediate mass Herbig Ae (HAe) stars are warmer (and generally more massive) analogs of those surrounding lower mass TTauri stars. Accurate disk orientation, sizes, temperatures, and CO abundances are available for a few objects only: AB Aur (Piétu et al. 2005), MWC 480 (Simon et al. 2000; Piétu et al. 2007), and HD 163296 (Isella et al. 2007) have been studied in CO isotopologues, all having relatively massive and extended disks. However, the transition between Class II object (where the protoplanetary disk is made of gas and dust) and Class III (where the disk contains mainly dust) is poorly known. To study this transition phase between Class II and Class III, we observed the low mass disks around two intermediate mass pre-main-sequence (PMS) HAe stars CQ Tau and MWC 758.

2 Observations and data analysis

We have studied CQ Tau and MWC 758, two HAe ($\sim 2 M_{\odot}$) located at about 140pc in the Taurus complex. The disk around CQ Tau has been imaged at different wavelengths. So far, this is one of the oldest HAe star (~ 10 Myrs) surrounded by a resolved dust and gas disk (Mannings & Sargent 1997; Testi et al. 2001). Moreover, CQ Tau appears as a peculiar HAe star exhibiting an UX Ori like variability (Natta et al. 1997). The disk around MWC 758 has also been barely resolved in CO by Mannings & Sargent (1997, 2000). Both disks appeared significantly weaker and smaller in CO lines than the previously studied disks around HAe stars.

We have observed CQ Tau and MWC 758 in ^{12}CO J=21 line and 1.3mm continuum with the IRAM array (1.5" angular resolution) see figure 1. MWC 758 was also imaged in ^{12}CO J=10 (2.5" resolution). The data were fitted in the uv plane using a standard flaring disk model, with power-law distributions for all primary quantities (surface density $\Sigma(r) = \Sigma_0(r/r_0)^{-p}$, temperature $T(r) = T_0(r/r_0)^{-q}$, velocity $V(r) = V_0(r/r_0)^{-v}$, and scale height $H(r) = H_0(r/r_0)^{-h}$), following the method described in detail by Piétu et al. (2007). Results are presented in table.1. The disks are very similar, notably in size (200AU in CO) and mass ($1-3 \cdot 10^{-3} M_{\odot}$).

¹ Université Bordeaux 1, LAB, UMR 5804, 2 rue de l'Observatoire, BP 89,33270 Floirac, France

² CNRS/INSU - UMR 5804, BP 89, 33270 Floirac, France

³ IRAM 300, rue de la piscine 38406 Saint Martin d'Hères France

(1) Source Data	(2) CQ Tau		(3)	(4)	(5) MWC 758	(6)	(7)
	$^{12}\text{CO J=2}\rightarrow\text{1}$	Dust		$^{12}\text{CO J=2}\rightarrow\text{1}$	$^{12}\text{CO J=1}\rightarrow\text{0}$	^{12}CO	Dust
V_{LSR} (km.s $^{-1}$)	6.17 ± 0.04			5.79 ± 0.01	5.90 ± 0.02	5.80 ± 0.02	
Orientation, PA ($^{\circ}$)	-36.7 ± 1.3	-36 ± 18		-31 ± 1	-23 ± 3	-31 ± 1	-38 ± 7
Inclination, i ($^{\circ}$)	29.3 ± 1.7	29 ± 9		18 ± 6	16 ± 1	16 ± 4	40 ± 20
Velocity(*), (km.s $^{-1}$)	4.0 ± 0.2			3.6 ± 1.1	[4.00]	4.0 ± 0.6	
Velocity exponent, v	0.51 ± 0.02			0.51 ± 0.03	0.47 ± 0.07	0.50 ± 0.02	
Stellar mass, M_{*} (M_{\odot})	1.8 ± 0.2			1.5 ± 0.7 [1.80]	[1.80]	1.80 ± 0.5	
Σ (*), (cm $^{-2}$)	$1.7 \pm 0.1 10^{16}$	$1.7 \pm 0.3 10^{22}$		$3.5 \pm 0.7 10^{16}$	$1.6 \pm 2.4 10^{16}$	$4.7 \pm 0.9 10^{16}$	$6.0 \pm 2.0 10^{22}$
Σ_{mass} (*), (g.cm $^{-2}$)		0.075 ± 0.015					0.3 ± 0.1
Exponent p	2.3 ± 0.2	1.3 ± 0.1		2.7 ± 0.5	[3]	2.9 ± 0.4	1.5 ± 0.4
Outer radius R_{out} , (AU)	200 ± 20	200 ± 30		300 ± 20	230 ± 30	270 ± 15	180 ± 40
Temperature(*), (K)	150 ± 50 [150]			37 ± 6	24 ± 4	30 ± 1	
Exponent q	0.7 ± 0.5 [0.5]			0.05 ± 0.20	0.6 ± 0.3	0.37 ± 0.15	
δV (*), (km.s $^{-1}$)	0.32 ± 0.09			0.50 ± 0.03	0.28 ± 0.10	0.44 ± 0.02	
Scale height(*), (AU)	22			15		11	
β		0.70 ± 0.04					1.0 ± 0.15

Table 1. Best parameters. Column (1) contains the parameter name. Columns (2) and (4) indicate the parameters derived from $^{12}\text{CO J=2}\rightarrow\text{1}$, column (5) parameters derived from $^{12}\text{CO J=1}\rightarrow\text{0}$, and columns (3) and (7) parameters derived from the dust emission, using the disk temperature from ^{12}CO and the dust emissivity from $\kappa_{\nu}(\nu) = 0.1(\nu/10^{12}\text{Hz})^{\beta}\text{cm}^2\text{g}^{-1}$ (Beckwith et al. 1990). Column (6) indicates the results of a simultaneous fit to both CO lines. Note that the P.A. is that of the disk axis. δV is the local line width (sum of thermal + turbulent component see Pietu et al. 2007 for a description of the convention). Σ is the surface density ($(\text{H}+2\text{H}_2)/2$) and Σ_{mass} the mass surface density assuming a g/d ratio of 100. (*) values at 100 AU. Square brackets indicate fixed parameters. The error bars correspond to 1 σ level of uncertainties.

Note that the masses are quite low comparing to the standard T Tauri disks ($\sim 10^{-2}M_{\odot}$). Both disks are in Keplerian rotation. The dust emissivity spectral index ($\beta = 0.7-1$) indicates that grain growth has occurred in those sources. One surprising result is the low CO abundance ($\sim 10^{-6}$ instead of the standard value of 10^{-4}) assuming the standard value of 100 for the gas-to-dust ratio (g/d) i.e., CO is depleted by a factor of about 100. Although the two sources are quite similar, CQ Tau is hotter and less dense by a factor 5 than MWC 758.

The high CO depletion suggests that the g/d ratio may be much lower than our assumed value of 100 because we are observing disks in the process of dissipating their gaseous content. Since the temperature of these two disks is large, depletion of CO due to sticking on grains cannot be invoked in a simple way.

3 Chemistry modeling

We use the PDR code from the Meudon group (Le Petit et al. 2006 and reference therein) to study the chemistry of the disks. The model is a 1D stationary plane-parallel slab of gas and dust illuminated by an ultraviolet (UV) radiation field. We use a chemical network similar to that of Goicoechea et al. 2006. No freeze-out onto grains is considered. We take into account a power-law grain size distribution $n(a) \propto a^{-\gamma}$ following HilyBlant et al. 2009 with a_+ and a_- being the maximum and minimum cutoff radii, respectively. The resulting extinction curve is calculated using the Mie theory for homogeneous isotropic spherical particles. To have a two-dimensional molecular distribution we compute the model at different radii in the disk. The output of this 1+1D model is the vertical distribution of molecular abundance calculated at different radii. As an input, we impose temperature and vertical density laws as derived from Table 1 at each radius. We investigate several g/d ratio (10–100 to mimic gas dispersal) under various UV field conditions (Draine field with a scaling factor $\chi = 10^3-10^4$), and different maximum grain size ($a_+=1\mu\text{m}-1\text{mm}$ to mimic grain growth). The dust mass is constant in all our simulations. The thermal balance is calculated. The results for the CQ Tau structure are presented on figure 3.

4 Discussion

Figure 3 (bottom) suggests that a case with $a_+ \geq 1\text{mm}$ and $g/d \simeq 100$ can explain CO column densities of the order of 10^{16}cm^{-2} around 200AU for CQ Tau. Figure 3 (top) allows us to conclude that the case with $a_+ = 1\mu\text{m}$ cannot explain the observed CO column densities, even with a low g/d ratio. For CQ Tau this is in agreement with the spectral index we measure ($\beta = 0.7$), which indicates that significant grain growth has occurred as also found by Testi et al.2003. This result suggests that grain growth, or more precisely the enhancement of the UV

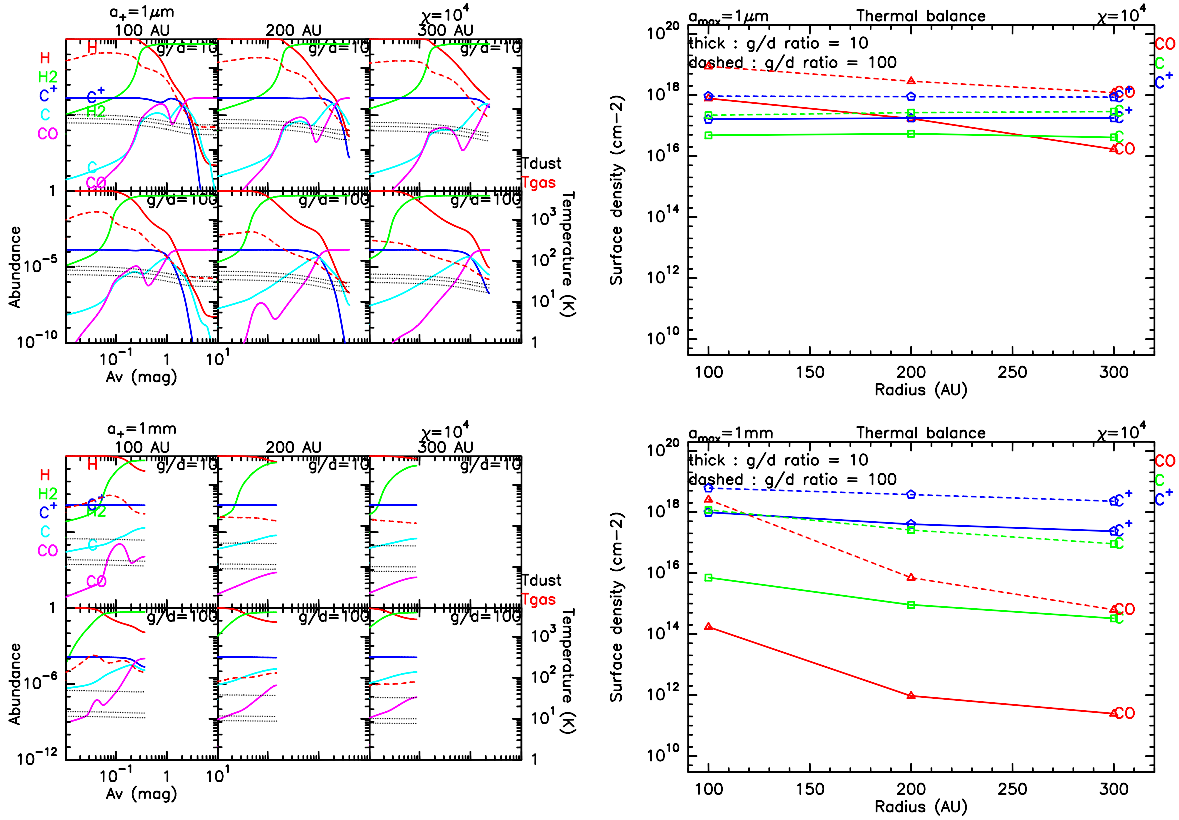


Fig. 1. Left: Vertical distribution through the disk of the abundance of H , H_2 , C^+ , C and CO and gas (dashed line) and dust (dotted line) temperature at the radii 100, 200 and 300 AU for the models with standard UV field ($\chi = 10^4$ at 100 AU), $a_+ = 1\mu\text{m}$ (top) and $a_+ = 1\text{mm}$ (bottom). Dust temperature is plotted for three grain sizes: a_+ , a_- and $(a_+ + a_-)/2$. **Right:** Radial distribution of the surface density of C^+ , C and CO for the model with standard UV field ($\chi = 10^4$ at 100 AU), $a_+ = 1\mu\text{m}$ (top) and $a_+ = 1\text{mm}$ (bottom).

penetration resulting from grain growth, is the dominant process explaining the measured CO column density. The observed CO temperature and the temperature calculated from the (approximate) thermal balance are in reasonable agreement for CQ Tau, around 60 – 100 K.

MWC 758 poses a different challenge, as the observed gas temperature is much lower, about 30 K, while the estimated CO column density is similar. Taken at face value, the results of the thermal balance study would favor the low g/d ratio solution (i.e., $g/d = 10$), which results in a somewhat more efficient cooling. However, there are several significant uncertainties in our modeling procedure. For example, the amount of small grains which controls the photo-electric heating is poorly constrained, and therefore the efficiency of this process may be overestimated in our model. Similarly, the gas-grain coupling is dominated by the small grains, because of their larger cross section and higher temperature, and remains also rather uncertain. Furthermore, we use a simple approximation for the diffusion of UV photons toward the disk plane, and even the unattenuated UV flux is uncertain. Note that the photodissociation is totally dominated by the UV excess (900–1200Å see Figure 2), while the stellar UV flux will play a role in the heating processes.

A totally different alternative to explain the low CO -to-dust ratio resides in the thermal history. Although the observed CO gas (and presumably small dust) is too warm to allow efficient sticking to grains, we find that the temperature of large grains can be low enough to prevent CO from being released from the grain surfaces.

In any case, our study clearly indicates that a low apparent CO abundance does not necessarily imply a low gas-to-dust ratio, and thus that CO is not an unambiguous tracer of this ratio.

Besides, the accurate determination of the inclination of CQ Tau ($29^\circ \pm 2$) challenges the UX ori hypothesis for this source since this phenomenon requires that the disk inclination to be larger than $\sim 45^\circ$ (Natta & Whitney 2000). Moreover, Eisner et al. 2004 have measured the inclination of the inner disk axis in near infra-

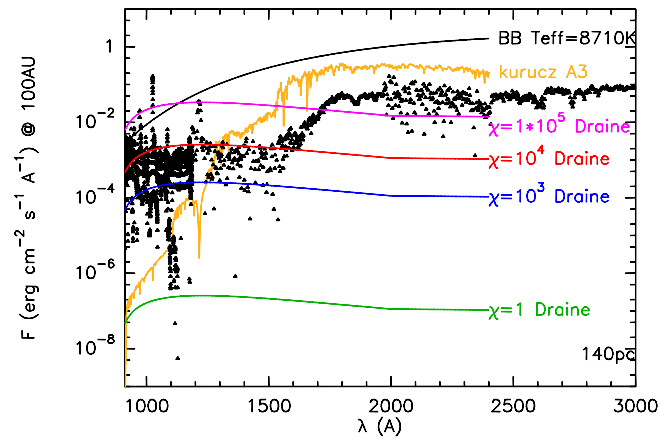


Fig. 2. Flux at 100 AU of FUSE and IUE observations MWC 758 (points), an A3V star according to the Kurucz atlas, a black body with the same temperature as an A3 star and several scaled Draine fields. The curved labeled 10^5 is calculated to have the same integrated intensity between 912 and 2400 Å as the observations. The star is assumed to be at 140 pc.

red. They found $48 \pm 5^\circ$. This result suggests that the disk may be warped by dynamical interactions with (yet undetected) inner bodies, but such large warps have never been observed so far.

More details about this study can be found in Chapillon et al. 2008

We acknowledge all the PdBI IRAM staff, Pierre Hily-Blant, Franck Le Petit, Thierry Forveille, Gail Schaeffer and Claire Martin-Zaïdi. This research was supported by the INSU program PCMI.

References

- Beckwith, S.V.W., Sargent, A.I., Chini, R.S., & Guesten, R. 1990, *AJ*, 99, 924
 Chapillon, E., Guilloteau, S., Dutrey, A., & Piétu, V. 2008, *A&A* 488, 565, 578
 Eisner, J.A., Lane, B.F., Hillenbrand, L.A., Akeson, R.L., & Sargent, A.I. 2004, *ApJ*, 613, 1049
 Goicoechea, J.R., Pety, J., Gerin, M., et al. 2006, *A&A*, 456, 565
 Grady, C.A., Woodgate, B.E., Bowers, C.W. et al. 2005, *ApJ*, 630, 958
 Hily-Blant, P., Dartois, E., Dutrey, A., et al. 2009 (*A&A* submitted)
 Isella, A., Testi, L., Natta, A., et al. 2007, *A&A*, 469, 213
 Le Petit, F., Nehmé, C., Le Bourlot, J., & Roueff, E. 2006, *ApJS*, 164, 506
 Mannings, V., & Sargent, A.I. 1997, *ApJ*, 490, 792
 Mannings, V., & Sargent, A.I. 2000, *ApJ*, 529, 391
 Natta, A., Grinin, V.P., Mannings, V., & Ungerechts, H. 1997, *ApJ*, 491, 885
 Natta, A., & Whitney, B.A. 2000, *A&A*, 364, 633
 Piétu, V., Guilloteau, S., & Dutrey, A. 2005, *A&A*, 443, 945
 Piétu, V., Dutrey, A., & Guilloteau, S. 2007, *A&A*, 467, 163
 Simon, M., Dutrey, A., & Guilloteau, S. 2000, *ApJ*, 545, 1034
 Testi, L., Natta, A., Shepherd, D.S., & Wilner, D.J. 2001, *ApJ*, 554, 1087